07

Macroscopic quantum phenomena under conditions of deposition of DNA oligonucleotides into the edge channels of a silicon nanosandwich structure

© M.A. Fomin,[1] P.A. Golovin,[1] L.E. Klyachkin,[1] A.M. Malyarenko,[1] A.K. Emelyanov,[2] N.T. Bagraev[1]

[1] Ioffe Institute,
194021 St. Petersburg, Russia
[2] St. Petersburg Nuclear Physics Institute, National Research Center Kurchatov Institute,
188300 Gatchina, Leningrad Region, Russia
e-mail: fomin.makseem@gmail.com

Received February 22, 2024 Revised July 4, 2024
Accepted July 15, 2024

The role of DNA oligonucleotides in the quantum transport of carriers using the edge channels of a silicon nanosandwich structure has been studied. Macroscopic quantum effects were discovered within the framework of a quantum analogue of the Faraday electromagnetic induction effect, demonstrating the interconnection of the characteristics of quantum interference occurring in edge channels involving a biomolecule. In particular, the fractal nature of quantum interference was demonstrated in the dependences of the longitudinal and transverse conductance staircases of a nanosandwich structure under conditions of DNA oligonucleotide deposition on the surface of edge channels.

Keywords: quantum interference, DNA identification, quantum Hall effect, Shubnikov–de Haas oscillations, quantum conductance staircase, electromagnetic Faraday induction.

DOI: 10.61011/TP.2024.09.59298.44-24

Introduction

Richard Feynman in his lecture „There's Plenty of Room at the Bottom: An Invitation to Enter a New Field of Physics" suggested in in 1959 that it is possible to mechanically move single atoms using a manipulator of the appropriate size, at least such a process would not contradict the physical laws known at that time [1]. At that time, he considered this approach as a more powerful form of synthetic chemistry, but the very idea of obtaining and using nanoscale particles in various applications was picked up by scientists and accepted for implementation. So, the field of science of nanotechnology appeared towards the end of the XX century.

As is known, the phenomenon of quantum interference manifests itself in many quantum macroscopic effects. From this point of view, its properties can be studied using subatomic objects, which can be a biological object of appropriate size, for example: bacteria — their size ranges from $0.1-10\,\mu$m, corresponding to the mesoscopic scale; viruses — usually $10-200$ nm, this is the upper nanometer range; proteins — from 4 to 5 nm, the lower nanoscale; DNA — a double helix with a diagonal of the order of 2 nm and an internucleotide distance of 0.34 nm (Fig. 1), where the nucleotide is the „building block" of nucleic acids (DNA, RNA), which come in 4 types and consist of a nitrogenous base, pentose and a phosphate group [2]. The sequence of nucleotides is called an oligonucleotide, and its length is the length of the persistence. While the width of an oligonucleotide is fixed, it can have any length depending on the number of base pairs (the so-called pair of nucleotides with each of the helices connected by a hydrogen bond according to the principle of complementarity) in it.

Thus, DNA is most suitable for the role of auxiliary quantum-dimensional particles from biological objects, the size of which can also be varied by synthesizing oligonucleotides of different lengths. It should be noted here that the study of the behavior of a biological object on the surface of a two-dimensional electronic system is interesting both from the point of view of studying its contribution to the parameters of observed quantum macroscopic phenomena and the features of the biomolecule itself.

At the same time, there is a need to create an alternative method for DNA sequencing - the technology of nucleotide decoding of the primary DNA structure. In recent years, molecular diagnostics and life sciences have developed rapidly, largely due to the creation of new methods for detecting nucleic acids. First of all, the main result of technological progress was the creation and development of new generation sequencing methods [3–8], based on the application of physical research principles, primarily — this is the detection of a response from a modified fluorescent or radioactive nucleotide label. At the end of the DNA sequencing process, a description of the primary structure of a linear biomolecule is obtained in the form of a sequence of nucleotides in text form. It should be said that the vast majority of technologies for deciphering the structure of DNA oligonucleotides are extremely expensive due to the use of complex optical circuits, while the

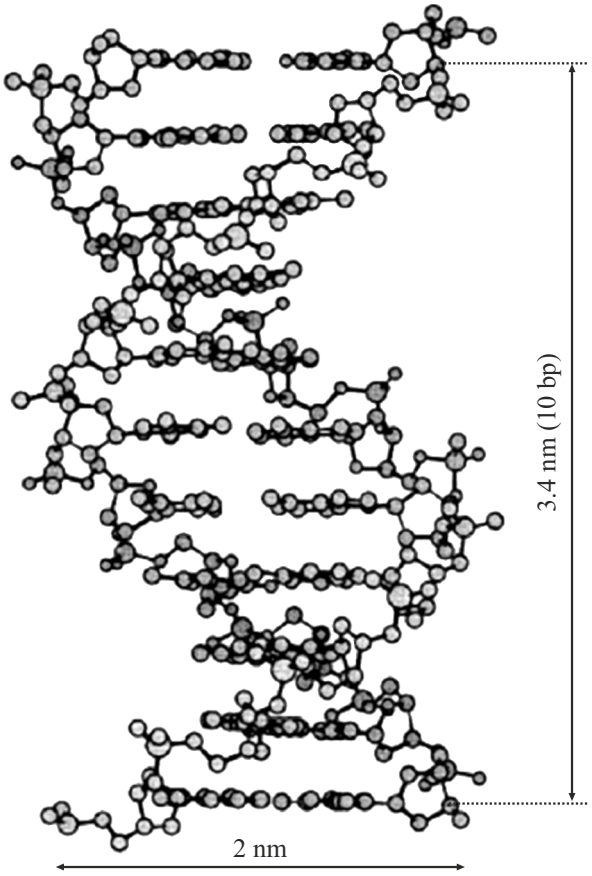

Figure 1. The diagram of the double spiral of the DNA oligonucleotide. The width of the oligonucleotide is plotted on the horizontal axis and length is plotted on the vertical axis which in this case is 3.4 nm (0.34 nm·10 base pairs).

use of markers to identify specific nucleotides introduces errors in the research results — such methods of indirect, indirect detection are characterized by high complexity of sequencing biomolecules with a huge number of repeating elements [4,5]. Thus, the task of creating alternative methods for identifying the primary structure of biomolecules remains highly relevant.

It should be noted here that it is possible to identify the properties of oligonucleotide sequences as a whole [9–12] — if we consider the sequence of nucleotides as a whole object. This approach implies the analysis of the physical features of oligonucleotide molecules, primarily the study of their role in the transport of carriers of the structure on the surface of which they are studied. It makes sense to use quantum-dimensional structures here, since the oligonucleotide itself has nanometer dimensions.

Although quantum mechanics studies microscopic objects of atomic and subatomic scales, some macroscopic phenomena are explained precisely within its framework. These include effects related to dimensional quantization, Landau quantization, for example, the Shubnikov–de Haas and de Haas–van Alphen oscillations, because it was Landau who first noticed the important role of macroscopic quantum effects. It should be noted that these phenomena are described by the characteristics of the macrocosm, i.e. it is possible to obtain the dependence of macroscopic parameters on quantum phenomena under certain conditions. The most important of them is the so-called strong field condition, $\omega_c\tau \gg 1$, where τ — relaxation time, $\omega_c = \frac{eH}{cm^*}$ — cyclotron frequency, e and m^* — charge and effective mass of the carrier, H —magnetic field strength, and c — the speed of light in vacuum. A long relaxation time is required to comply with it, which is greatly reduced due to the electron-electron interaction (especially at the boundaries of the quantum system), as a result of which it is assumed that the described macroscopic quantum phenomena should be studied at extremely low temperatures. It also requires a small amount of effective carrier mass, which was difficult to achieve at the dawn of quantum mechanics, and for this reason large magnetic fields were used. Accordingly, the phenomena associated with Landau quantization are traditionally limited by low temperatures and high magnetic fields, which is associated with the negative influence of the electron-electron interaction. However, these restrictions can be mitigated by increasing the relaxation time and reducing the effective mass.

Based on the above, one of the tasks of this work was to create conditions for the suppression of electron-electron interaction and localization of sample carriers within the framework of registration of the quantum Hall effect. In this regard, topological systems with edge channels are of interest, the properties of the boundaries of which should contribute to the suppression of electron-electron interaction. The fact is that the topological insulators in which these edge channels are formed are characterized by the presence of surface or edge states formed due to the disappearance of the band gap in the energy spectrum of the structure [13]. Moreover, edge channels are equivalents of ballistic conducting channels and are formed by pairs separated in space, the carriers in which have the opposite orientation of spins in the effective absence of an external magnetic field, which makes it possible to observe spin-dependent phenomena, in particular, the quantum spin Hall effect [13,14].

It is important to say that, although the structures described above make it possible to suppress the electron-electron interaction to a greater extent, there is still the problem of the negative contribution of the boundaries of low-dimensional structures to this phenomenon. So, recently, approaches to solving this problem have been developed, based on the exchange interaction of carriers with the boundaries of the quantum system — it allows saving the moment and energy of the carriers. As examples of the described technique, it is worth noting the creation of shells at the boundaries of f- and d-elements [15], as well as from dipole centers with negative correlation energy „negative-U“, ($2D^0 \rightarrow D^- + D^+$) [16,17]. At the same time, the option with dipole centers allows experiments to be

carried out at high temperatures, up to room temperature, due to the negative-U reaction.

Therefore, it is of interest to use systems with negative correlation energy, as a result of which a silicon nanosandwich structure (SNS) is used as a sample in this paper, which has edge channels limited by boron dipole centers with negative correlation energy, contributing to the transport of single carriers under conditions of suppression of electron-electron interaction [18]. Moreover, the carriers in the edge channels of the SNS have a low effective mass and a long relaxation time, and due to the strong suppression of the electron-electron interaction in the edge channels, they form separate sequential quantum harmonic oscillators, the so-called „pixels", containing single carriers, the transport of which along the dipole centers of the edge channels is quantum [19].

Moreover, in the case of working with a lattice scheme, the possibility of observing an electrical equivalent of the quantum Hall effect is of interest, which can be described by the quantum Faraday effect, which implies the use of the Laughlin's model for quantum particle transport in the absence of an external magnetic field [20]. Here we mean a situation where magnetic lattices are created by the passage of the source−drain current I_{ds} through a sample of a heterostructure, thereby inducing a magnetic field, the quanta of the magnetic flux of which are captured by single sample carriers, which as a result of the quantum analogue of the Faraday electromagnetic induction effect results in the generation of new current in the edge channel:

$$I_{gen} = \frac{dE}{d\Phi} = \frac{n_e eU}{n_\Phi \Delta\Phi},$$

where n_e and n_Φ — the number of holes and magnetic flux quanta involved in the process, $\Delta\Phi = \Delta BS$, S — the effective area of the edge channel of the SNS, and $\Delta B = I_{ds}/2R_0$, where $R_0 = \sqrt{\frac{S}{\pi}}$ — the effective radius of the quantum harmonic oscillator, i.e. pixels with an area of S in our case.

It is known that the quantum Hall effect can be observed in SNS within the framework of the standard approach, i.e., by applying an external magnetic field to the sample, this approach is described in Ref. [21]. If we use a quantum equivalent of Faraday's electromagnetic induction, then an external magnetic field is not required to observe the quantum Hall effect, since the passing stabilized source−drain current induces its magnetic field, which eventually still results in the occurrence of the voiced macroscopic quantum phenomenon. This fact makes it possible to control the quantization value of the Hall resistance by varying I_{ds}, which, in turn, makes it possible to describe the observed quantum Hall effect as its electrical equivalent. Such a model was used to identify macroscopic quantum phenomena in this study.

All of the above results in the fact that today it is of great interest to solve the problem of studying the contribution of DNA oligonucleotides to the quantum properties of carrier transport of quantum-dimensional systems, in particular, the influence of biomolecules on the effect of quantum interference underlying various quantum macroscopic phenomena. The study method chosen in this paper was the study of the quantum Hall effect and the quantum staircase of longitudinal conductance under conditions of deposition of DNA oligonucleotide on the surface of the SNS, for the description of which a quantum equivalent of the Faraday electromagnetic induction effect was used in this paper.

Indeed, quantum macroscopic phenomena such as equivalents of the quantum Hall effect and Shubnikov−de Haas oscillations, quantum staircases of longitudinal conductance were discovered in the course of study of the properties of the edge channels of the SNS in the framework of this paper. The data obtained indicate a multilevel structure of quantum interference in the SNS — oligonucleotide system.

1. Experimental procedure

The SNS is an ultra-narrow quantum well of p-type conductance (p-type self-ordered silicon quantum well), bounded by two delta barriers strongly doped with boron ($5 \cdot 10^{21}$ cm^{-3}), on the surface of n-silicon (100) [18,22,23] (Fig. 2). Boron atoms in δ-barriers form trigonal dipole centers ($B^+ - B^-$) at such an ultrahigh concentration due to the negative-U reaction: $2B^0 \rightarrow B^+ + B^-$ with crystallographically oriented sequences forming the edge channels responsible for conductance in p-Si−QW. p-Si−QW edge channels are effective sources of THz and GHz radiation under longitudinal current conditions due to the presence of negative-U dipole centers of boron [18,24]. This allows the SNS to emit in the THz range, while being an extremely compact heterostructure due to the Josephson transition and multiple Andreeyev radiation at the edges of the pixel. At the same time, the SNS was performed within the framework of the Hall geometry.

The study of the SNS by various methods showed that the conduction channel responsible for conductance consists of a sequence of „pixel" — embedded self-ordered microresonators containing a single hole inside due to a $p-n$-transition in the depth of the structure tunneling through a sequence of boron dipole centers bounding it (pixel).

The model of carrier transport in the edge channel demonstrates quasi-one-dimensional sequences of Bohr dipole centers bounding the edge channels of the SNS, and two counter Josephson transitions at the interface between opposite pixel boundaries. Under these conditions, suppression of the electron-electron interaction is observed due to sufficiently long spin-lattice relaxation times, $\tau \cong 7 \cdot 10^{-10}$ s, for light holes $\tau \cong 5 \cdot 10^{-10}$ s, for heavy holes — $\tau \geq 5 \cdot 10^{-10}$ s. This results in a high level of carrier mobility in the edge channel, of the order of $\mu \geq 200\,\mathrm{m}^2/(\mathrm{V}\cdot\mathrm{s})$ [18,25,26]. It is shown that the presence of boron dipole centers results in a decrease of the intensity of the electron-electron interaction due to the exchange

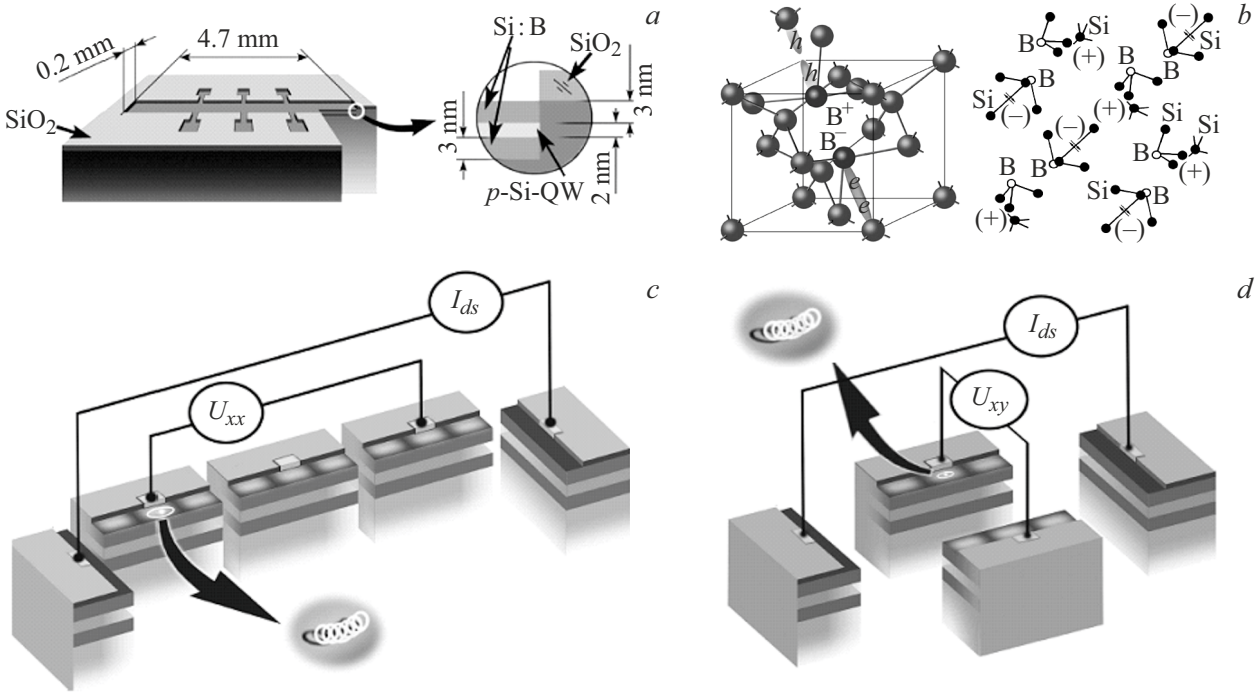

Figure 2. *a* — schematic representation of the SNS with indication of the dimensions of the conduction channel and the thickness of the layers in which *p*-type self-ordered silicon quantum well and δ-barriers limiting it are located; *b* — images of the trigonal dipole center of boron (B^+ B^-) and their self-ordered chains bounding *p*-type self-ordered silicon quantum well; *c, d* — schematic representation of contacts on SNS in the section from which the longitudinal U_{xx} (*c*) and transverse U_{xy} (*d*) current-voltage curve was measured in the conditions of passage of the stabilized source−drain current, I_{ds}. The place of deposition of the oligonucleotide on the surface of the SNS, namely on the edge conduction channel, is also indicated.

interaction of holes with them. The spin-dependent carrier transport was also studied in the edge channels of the SNS, as a result of which the spin polarization of holes was discovered. It was shown that ballistic carrier transport takes place in the edge channels [27]. The registration of Aharonov−Kasher oscillations in the dependences of the longitudinal conductance on the gate voltage showed the presence of spin interference due to the presence of spin polarization of carriers, and at sufficiently high temperatures, due to trigonal dipole centers with negative correlation energy. This is very reason why it is possible to observe various quantum macroscopic phenomena associated with dimensional quantization in the SNS.

The DNA oligonucleotides used in this work were synthesized using automatic nucleotide synthesizer K&A (Germany). The accuracy of the obtained result, namely the number of base pairs in the sequence, was confirmed using mass spectral analysis. Subsequently, the oligonucleotides were purified in polyacrylamide gel and HPLC using ZORBAX chromatographic columns produced by Agilent (USA) designed for the separation of oligonucleotides. Specially prepared water and solutions free of DNA bases and chemical impurities were used at all stages of purification. The length of the obtained oligonucleotides was rechecked after completion of purification using agarose gel electrophoresis, which confirmed the correctness of DNA synthesis.

The following double-stranded nucleotide sequences were synthesized within the framework of the above-described technique:

100 b. p.: 5'-ctggtgggtg tggacgccct gatgatcgtc actggcctca tcggagcctt gagccacacg gccatagcca gatacagttg gtggttgttc tctacaattt-3'

Oligonucleotide molecules were precisely deposited on the δ-barrier above the edge channels of the SNS using a microdosator and a microfluidic container-type system made of polydimethylsiloxane placed on the surface of the SNS [23]. At the same time, oligonucleotides were deposited according to the scheme of 1 oligonucleotide−1 pixel, which corresponds to 1 hole. This technological process was well described in Ref. [23,28]. The corresponding concentration was selected, which was equal to $1.96\,\mu g/\mu l$ under conditions of two-dimensional hole density of $3 \cdot 10^{13}\,m^{-2}$ (Hall measurements [22]). In turn, the carrier density also determines the number of pixels that make up the edge conductance channel of the SNS: for example, the segment between the contacts „xx" with a length of 2 mm accommodates $\sim$ 120 pixels, since each harmonic oscillator (pixel) containing a single hole, has a length of $16.6\,\mu m$.

The current-voltage curves (CVC) of the SNS were recorded in this paper, namely, the longitudinal and trans-

verse components of the SNS voltage under conditions of deposition of DNA oligonucleotide on the surface of the edge channels. The stabilized source−drain current was supplied in the range $(-50)-(+50)\,\mu$A, each point was measured 10 times with an interval of 1 ms. The voltages described in the paper were removed from the contacts „xx“ (Fig. 2, *c*) and „xy“ (Fig. 2, *d*). The experiment was performed at room temperature, and the experimental setup consisted of a system consisting of current source Keithley 6221, nanovoltmeter Keithley 2182a, a PC and a SNS, the contacts of which were connected to the coaxials of a shielding container, inside which a nanostructure with a deposited DNA oligonucleotide sample was placed. The system was synchronized and controlled using the LabVIEW program.

2. Experiment and results obtained

The measurement result was the recording of the longitudinal and transverse CVC of the SNS under conditions of deposition of DNA oligonucleotide on the surface of the edge channels (Fig. 3, *a, b*). Repeated stress peaks are visible on the obtained dependencies, and their periods for the longitudinal and transverse components are equal to each other. Moreover, a similar pattern is observed inside each peak in case of zooming in: for instance, more peaks are visible in Fig. 3, *c, d*, they are smaller in magnitude, but still have a certain periodicity. At the same time, these peaks within the peaks are repeated on both sides, and their periods are also approximately equal. It is worth remembering here that our edge channel, as shown earlier, is a sequence of holes localized in space, i.e. a system of quantum harmonic oscillators (pixel) of a certain length of 16.6 μm each. Also, the deposition of a DNA oligonucleotide in such a way that each pixel corresponds to one biomolecule was one of the conditions of the experiment.

Therefore, the thesis of this paper is that the peaks obtained in this experiment on the CVC can demonstrate several levels of quantum interference, i.e. interference on different circuits: the largest peaks correspond to interference in the section of the edge channel between the contacts „xx“, the smaller peaks correspond to interference on a single pixel, and the smallest peaks which are visible in Fig. 3, *e, f*, correspond to interference on oligonucleotide. At the same time, the oscillation periods are different in each of these cases, since the size of the interference contour is different: the segment „xx“ consists of 120 pixels, the pixel itself has a length of 16.6 μm, and the length of the of 100 base pair (b. p.) oligonucleotide used in this paper is 34 nm. Let's now focus on each case in more detail.

Let us first consider the obtained dependences of the CVC on the stabilized source−drain current in the entire spectrum of $(-50)-(+50)\,\mu$A. In this case, it is stated that quantum interference is observed in the section of the edge channel between the contacts „xx“. The dimensions of this section consisting of a sequence of pixels are known: the length is 2 mm, and the width is 2 nm, since this is the width of pixels. The SNS CVC obtained in the paper have an oscillatory character, while the periods of these oscillations coincide for cases of longitudinal and transverse stresses. These features suggest the quantization of the corresponding conductivities due to quantum dimensional effects, however, there was no external magnetic field in the experiment. Nevertheless, this fact is offset if we apply the above-described model of the quantum equivalent of Faraday electromagnetic induction, in which the passage of the stabilized source−drain current induces a magnetic field. In this case, it becomes possible to observe quantum macroscopic phenomena in the SNS, for instance, the quantum Hall effect, since the dependence of the longitudinal conductance on the magnetic field induced by the source−drain current can be considered as an electrical equivalent of the Shubnikov−de Haas oscillations, and the transverse resistance like the Hall resistance staircase. It remains to calculate and estimate the values of the Hall resistance and longitudinal conductance.

As mentioned above, the Faraday model of the quantum analogue of electromagnetic induction implies the induction of a magnetic field due to the passage of a stabilized source-drain current through the edge channels of the SNS, which constitute a closed LC circuit, which allows considering the obtained voltage values depending on the magnetic field. In this case, the Faraday EMF occurs which is experimentally measured at the Hall contacts „xy“:

$$\Delta U_{xy} = \frac{\Delta\Phi}{\Delta t},$$

where $\Delta\Phi$ — a change in the magnetic flux passing through the edge channels of the SNS, and $\Delta t = \frac{e}{I_{gen}}$, while I_{gen} — the current generated in this circuit by an induced magnetic field. In this case, the Hall resistance is determined primarily by the current I_{gen}:

$$\Delta R_{xy} = \frac{n_e \Delta U_{xy}}{n_\Phi I_{gen}}.$$

Here n_e and n_Φ is the number of holes and magnetic flux quanta captured by carriers in the edge channel, $\Delta\Phi$ is found by definition, $\Delta\Phi = \Delta B S$, while ΔB here is obtained from the ratio of the passing stabilized source−drain current, I_{ds}, to the effective radius of the quantum harmonic oscillator, R_0, being a pixel. Thus, $\Delta B = \frac{\Delta I_{ds}}{2R_0}$, where $R_0 = \sqrt{\frac{S}{\pi}}$, and S is the effective area of the contour to which the magnetic flux quanta are captured. In this case, a section of the sequence of 120 pixels is used between the contacts „xx“. It is worth noting here that $\Delta\Phi$ was calculated based on the thesis that one of the experimental conditions was the mode of 1 pixel−1 oligonucleotide. This meant that the oligonucleotide could divide the effective pixel area in half, since the biomolecule lies in the middle of the pixel, and the carrier inside it oscillates from the pixel wall to the

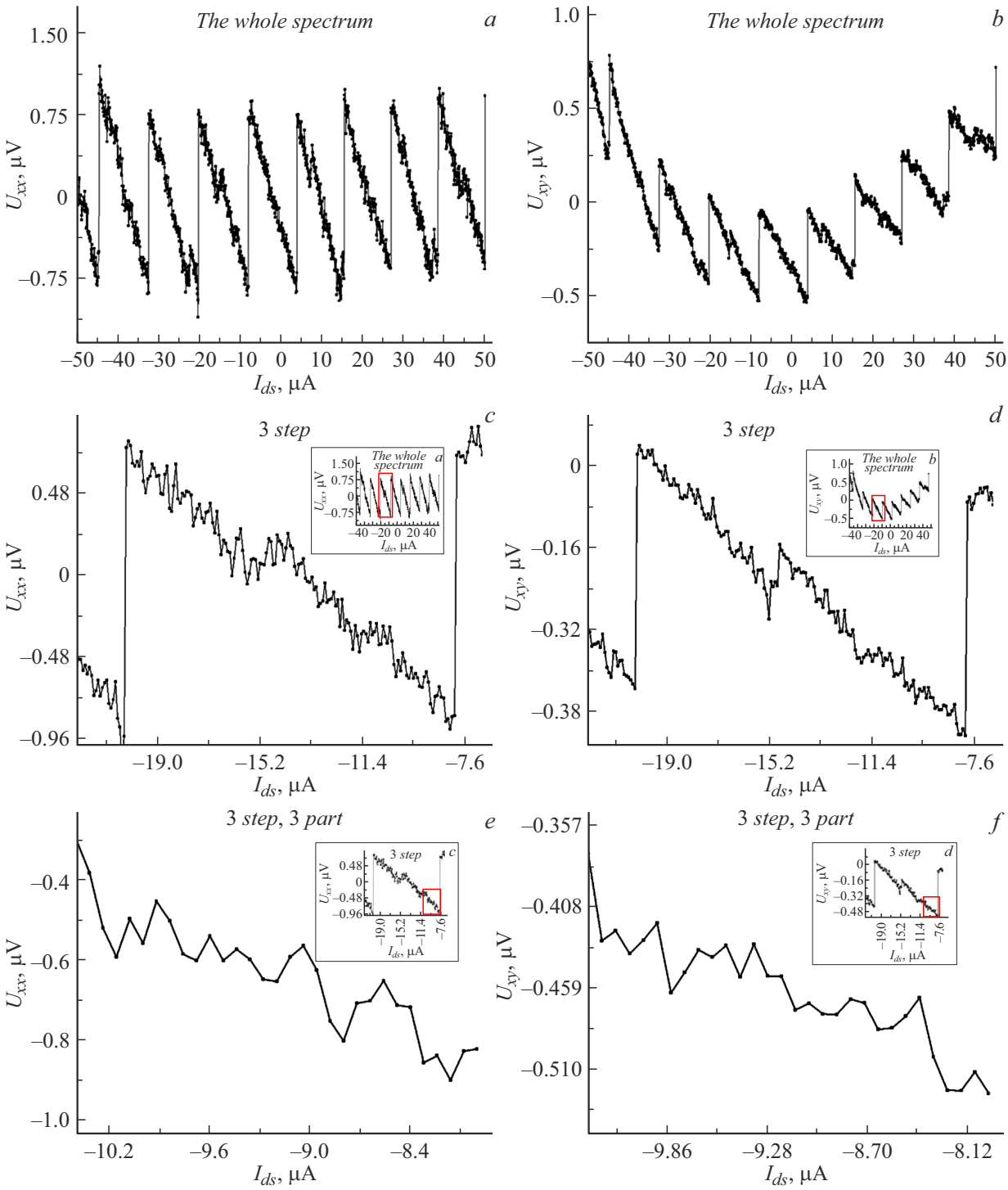

Figure 3. SNS current-voltage curves under conditions of deposition of a double-stranded DNA oligonucleotide with a length of 100 b. p. on the surface of the edge channels: *a, c, e* — longitudinal voltage from pulling stabilized current I_{ds}; *b, d, f* — transverse from I_{ds}. *a, b* — the first stage of interference (at the site „xx"); *c, d* — the second stage of interference (at a single pixel); *e, f* — the third stage of interference (on DNA oligonucleotide). The inserts show a section of the obtained dependencies of the previous interference stage, from where the current one was taken.

oligonucleotide and back. As it turned out, it really can be possible because a similar model was identified as a special case in an experiment with the removal of the magnetic susceptibility of the SNS under conditions of deposition of DNA oligonucleotide on the surface of the edge channels [12].

The generation current turned out to be as follows in accordance with the above: $I_{gen} = \frac{e}{\Delta t} = \frac{e\Delta U_{xy}}{\Delta\Phi}$. Therefore,

it is possible to determine the value of I_{gen}, and hence $\Delta R_{xy} = \frac{\Delta U_{xy}}{I_{gen}}$. It should be borne in mind here that the direction of current along a pixel can be bidirectional, i.e. the Josephson transition and multiple Andreev reflection are accompanied by a change in the direction of movement of the carrier along a sequence of dipoles at the edges of the pixel or along neighboring pixels the carrier moves in different directions with a change in spin to the opposite. It turns out that the current goes both ways at once during generation, and since the contacts „xy" are located on the „jumper" of the edge channel, i.e. in its center, the current bypasses the contour of the edge channel twice. Thus, bearing in mind the serial connection of the pixel, it is necessary to multiply the value obtained above by the number of pixels that the generating current has passed to determine the real resistance R_{xy} in this case, i.e. double the amount around the perimeter, the length of which is 9.8 mm — this is 1180 pixels.

Now let us calculate ΔG_{xx}: $\Delta G_{xx} = \frac{I_{gen}}{\Delta U_x}$, however, it is worth noting that the voltage drop over the entire section „xx", ΔU_{xx} was taken into account here, while the pixels in this case are switched on in parallel; thus, the value obtained above should be divided by the number of pixels in „xx", i.e. by 120 to determine the conductance of one pixel in this segment, and also it is necessary to keep in mind that the generation current described by the above formula flows throughout the entire section „xx", i.e. by 120 pixels, since it is calculated from the area of the entire segment „xx". Thus:

$$\Delta G_{xx} = \frac{I_{gen}}{\Delta U_{xx} \cdot 120 \cdot 120}.$$

For instance, it is possible to calculate the magnitude of the change of longitudinal conductance, as well as Hall resistance and conductance for the first stage of quantum interference, i.e. in the area between the contacts „xx". These values were $\Delta G_{xx} = 0.6\,[e^2/h]$, $\Delta G_{xy} = 14.3\,[e^2/h]$ and $\Delta R_{xy} = 0.07\,[h/e^2]$ for the first stage, which is in the range $(-44.08-(-32))\,\mu$A.

Now let's look at the situation inside the large peaks, an example of which is shown in Fig. 3, *c, d*. It can be seen that peaks are also observed within one of the periods of the general spectrum, which is shown in Fig. 3, *a, b*. As in the first case, the periods between the longitudinal and transverse components of these peaks are approximately the same. It makes sense to carry out the same studies that were performed above. However, now let us proceed from the logic that quantum interference occurs on a single pixel, so a new current will be generated on it, and the effective area in this case will be equal to a pixel, or rather, its half, since the oligonucleotide located on the surface divides the oscillatory route of the hole inside in half — from the edge of the pixel to the biomolecule and back again. ΔR_{xy} will be calculated similarly, however, in the case of ΔG_{xx}, one of the divisions by 120 will be removed, since it was previously divided due to current generation at 120 pixels, now only one is considered. In this case, $\Delta G_{xx} = 18\,[e^2/h]$, $\Delta G_{xy} = 4.55\,[e^2/h]$ and $\Delta R_{xy} = 0.22\,[h/e^2]$.

The last case remains which is the quantum interference on the DNA oligonucleotide. Indeed, it is possible to detect the next peaks inside the peaks by scaling the obtained current-voltage curve again (Fig. 3, *e, f*). In this variant, the oscillation of the hole inside the pixels within the oligonucleotide is implied. The generation current in this case is likely to be the same as for pixels, since the current envelopes not only the oligonucleotide, but also the pixel. Otherwise, the calculation model remains the same, so the following results are obtained: $\Delta G_{xx} = 59\,[e^2/h]$, $\Delta G_{xy} = 25\,[e^2/h]$ and $\Delta R_{xy} = 0.04\,[h/e^2]$.

As can be seen, the results obtained within the framework of applying the Faraday model of the quantum analogue of electromagnetic induction to the experimental data of the SNS current-voltage curve under conditions of DNA oligonucleotide deposition showed rather close orders of values. The described tricks for calculating the part of the generating current that is involved at each stage of interference were applied, since in the framework of the experiment, the current-voltage curve was removed from only two contacts, between which lies a certain number of pixels. Ideally, this experiment should be carried out by taking data directly from pixels or even an oligonucleotide, but this is not possible at the moment. In this regard, it is necessary to resort to approximations, but even so the results obtained are consistent with the observed features.

Conclusion

The conducted studies of the SNS current-voltage curve under conditions of deposition of DNA oligonucleotides on the surface of edge channels within the framework of the quantum analogue of Faraday electromagnetic induction demonstrated the presence of several types of quantum interference, which are fractal in nature: in the area between the contacts „xx", on the pixel and on the DNA oligonucleotide. At the same time, the quantum interference of a single hole on an oligonucleotide was recorded for the first time. The possibility of application of the model of quantum equivalent of the Faraday electromagnetic induction effect is also confirmed, since it allows describing the values of conductance and resistance of the longitudinal and transverse components in the Hall geometry.

Funding

This study was carried out within the framework of budget financing of the Ioffe Institute of Physics and Technology.

Conflict of interest

The authors state that they have no conflict of interest.

References

[1] R.P. Feynman. Saturday Review, **April 2**, 45 (1960).
[2] A.N. Ogurtsov. *Bionanotekhnologiya, principy i primenenie* (NTU KhPI, Kharkov, 2012) (in Russian)
[3] E.R. Mardis. Annu. Rev. Anal. Chem., **6**, 287 (2013). DOI: 10.1146/annurev-anchem-062012-092628
[4] M.A. Quail, M. Smith, P. Coupland, T.D. Otto, S.R. Harris, T.R. Connor, A. Bertoni, H.P. Swerdlow, Y. Gu. BMC Genomics, **13**, 341 (2012). DOI: 10.1186/1471-2164-13-341
[5] W. Timp, A.M. Nice, E.M. Nelson, V. Kurz, K. McKelvey, G. Timp. Special Section on Nanobiosensors, **2**, 1396 (2014). DOI: 10.1109/ACCESS.2014.2369506
[6] International Human Genome Sequencing Consortium (IHGSC), Finishing the euchromatic sequence of the human genome, Nature, **431** (7011), 931 (2004). DOI: 10.1038/nature03001
[7] J. Liu, C. Liu, W. He. Current Organic Chem., **17** (6), 564 (2013). DOI: 10.2174/1385272811317060003
[8] C. Dekker, M.A. Ratner. Phys. World, **14** (8), 29 (2001). DOI: 10.1088/2058-7058/14/8/33
[9] M.A. Fomin, A.L. Chernev, N.T. Bagraev, L.E. Klyachkin, A.K. Emelyanov, M.V. Dubina. Semiconductors, **52** (5), 612 (2018). DOI: 10.1134/S106378261805007X
[10] M.A. Fomin, A.L. Chernev, L.E. Klyachkin, A.M. Malyarenko, N.T. Bagraev. Intern. Conf. On IRMMW-THz, 8874337 (2019). DOI: 10.1109/IRMMW-THz.2019.8874337
[11] K.B. Taranets, M.A. Fomin, L.E. Klyachkin, A.M. Malyarenko, N.T. Bagraev, A.L. Chernev. J. Appl. Phys., **125**, 225702 (2019). DOI: 10.1063/1.5083805
[12] M.A. Fomin, L.E. Klyachkin, A.M. Malyarenko, V.V. Romanov, N.T. Bagraev. ZhTF, **92** (7), 963 (2022) (in Russian). DOI: 10.21883/JTF.2022.07.52651.5-22
[13] M.Z. Hasan, C.L. Kane. Rev. Mod. Phys., **82** (4), 3045 (2010). DOI: 10.1103/RevModPhys.82.3045
[14] M. Buttiker. Science, **325**, 278 (2009). DOI: 10.1126/science.1177157
[15] A.A. Zyuzin, D. Loss. Phys. Rev. B, **90**, 125443 (2014). DOI: 10.1103/PhysRevB.90.125443
[16] P.W. Anderson. Phys. Rev. Lett., **34**, 953 (1975). DOI: 10.1103/PhysRevLett.34.953
[17] N.T. Bagraev, V.A. Mashkov. Sol. St. Comm., **51** (7), 515 (1984). DOI: 10.1016/0038-1098(84)91024-X
[18] N.T. Bagraev, A.D. Buravlev, L.E. Klyachkin, A.M. Malyarenko, V. Gelhoff, V.K. Ivanov, I.A. Shelykh. FTP, **36** (4), 462 (2002) (in Russian).
[19] N.T. Bagraev, D.S. Gets, E.N. Kalabukhova, L.E. Klyachkin, A.M. Malyarenko, V.A. Mashkov, D.V. Savchenko, B.D. Shanina. FTP, **48** (11), 1503 (2014) (in Russian).
[20] N.I. Rudder, P.A. Golovin, N.T. Bagraev, L.E. Klyachkin, A.M. Malyarenko. Nauchno-Tekhicheskie Vedomosti SPbGPU, **14** (4), 9 (2021) (in Russian). DOI: 10.18721/JPM.14401
[21] N.T. Bagraev, V.Yu. Grigoryev, L.E. Klyachkin, A.M. Malyarenko, V.A. Mashkov, V.V. Romanov, N.I. Rul. Low Temperature Phys., **43** (1), 110 (2017). DOI: 10.1063/1.4974190
[22] N.T. Bagraev, V.Yu. Grigoryev, L.E. Klyachkin, A.M. Malyarenko, V.A. Mashkov, V.V. Romanov. Semiconductors, **50** (8), 1025 (2016). DOI: 10.1134/S1063782616080273
[23] N.T. Bagraev, A.L. Chernev, L.E. Klyachkin, A.M. Malyarenko, A.K. Emelyanov, M.V. Dubina. Semiconductors, **50** (9), 1208 (2016). DOI: 10.1134/S1063782616090037
[24] N.T. Bagraev, L.E. Klyachkin, R.V. Kuzmin, V.A. Mashkov. Semiconductors, **46** (3), 275 (2012). DOI: 10.1134/S1063782612030049
[25] N.T. Bagraev, L.E. Klyachkin, A.A. Kudryavtsev, A.M. Malyarenko. FTP, **43** (11), 1481 (2009) (in Russian).
[26] W. Gehlhoff, N.T. Bagraev, L.E. Klyachkin. Mater. Sci. Forum, **196–201**, 467 (1995). DOI: 10.4028/www.scientific.net/MSF.196-201.467
[27] N.T. Bagraev, E.Y. Danilovsky, L.E. Klyachkin, A.M. Malyarenko, V.A. Mashkov. FTP, **46** (1), 77 (2012) (in Russian).
[28] A.L. Chernev. Avtoref. kand. diss. (SPbAU RAN, SPb., 2017) (in Russian)

Translated by A.Akhtyamov